Electronic structure and magnetic properties of dilute Fe alloys with transition-metal impurities

B. Drittler, N. Stefanou,* S. Blügel,† R. Zeller, and P. H. Dederichs
Institut für Festkörperforschung der Kernforschungsanlage Jülich, Postfach 1913, D-5170 Jülich, Federal Republic of Germany
(Received 23 February 1989)

We present *ab initio* calculations for dilute Fe alloys with 3*d* and 4*d* elements. The calculations are based on local-density approximation of density-functional theory and employ the Korringa-Kohn-Rostoker Green's-function method. Results are given for the densities of states, the local moments, and the magnetization oscillations around the impurities. A detailed comparison is made with measurements of the electronic specific heat, with neutron-scattering results for the moments of the impurity and the neighboring host atoms, and with magnetization measurements. Contrary to the case of Co and Ni alloys, the majority-spin band contributes most to the screening in the Fe alloys. This arises from the fact that the Fermi energy falls into the minimum of the minority-spin density of states. The results are in qualitative agreement with a proposed pseudogap theory and naturally explain why Fe alloys show such a complicated magnetic behavior.

I. INTRODUCTION

There exists a large amount of experimental information on the electronic and magnetic properties of Fe alloys. Especially, dilute Fe alloys have been studied by many methods such as magnetization measurements, nuclear magnetic resonance, Mössbauer effect, or neutron scattering. From a theoretical point of view the understanding of these alloys has not yet sufficiently advanced, despite the well-known fact that density-functional theory represents a reliable method to calculate the magnetic properties of transition metals from first principles. In the last few years considerable progress has been made concerning the local behavior of impurities in Fe. Especially noteworthy are the calculations by Akai, Akai, and Kanamori[1,2] and by Akai *et al.*,[3] who give a consistent picture of the local moments, hyperfine fields and spin-lattice relaxation times T_1 of impurities in Fe. Also the results of Leonard and Stefanou[4] as well as the recent results of Anisimov *et al.*[5] should be mentioned in this context. In contrast to these efforts for the calculation of the local properties of impurities in Fe, the present paper is mainly addressed to the changes of the host properties caused by the impurities. In addition to the local properties we calculate the charge and magnetization oscillations around the impurities and make a detailed comparison with the experimental information about these systems.

The behavior of disordered concentrated alloys has been studied using the coherent-potential approximation (CPA). Especially, the work of Hasegawa and Kanamori[6] being based on tight-binding models has led to a basic understanding of these alloys. Recently more sophisticated and fully self-consistent CPA calculations based on the Korringa-Kohn-Rostoker (KKR) method and density-functional theory have been performed for some Fe alloys, e.g., for *Ni*Fe by Johnson, Pinsky, and Stocks[7] and Akai,[8] for *V*Fe by Johnson, Pinsky, and Staunton,[9] whereas Akai *et al.*[10] studied several Ni and Co alloys. In these CPA calculations the response of the host atoms is only considered in an average way. No detailed information about the charge and magnetization oscillations, which are the aims of the present paper, can be obtained by this method.

Dilute Fe alloys show a more complicated behavior than dilute Ni or Co alloys. Basically this arises from the fact that, contrary to the "strong" ferromagnets Co and Ni, Fe is a "weak" ferromagnet since the majority-spin band is not completely filled. This has important consequences for the magnetic properties of dilute Fe alloys, e.g., none of the dilute Fe alloys falls on the main branch of the Slater-Pauling curve and no universal behavior as for the Ni and Co alloys is found experimentally.[11,12] Nevertheless there are also strong similarities between the Fe and the Ni and Co alloys. To clarify these differences and similarities is one purpose of our paper. The second purpose is to compare our calculated densities of states, local impurity moments, and magnetization changes of the host atoms with the large amount of experimental information on these alloys.

The outline of the paper is as follows. In Sec. II we present a short account of the theoretical method and some technical information concerning the calculations. In Sec. III we present results for the local densities of states of the impurities and for the changes of the total density of states due to one impurity. At the Fermi energy these changes are directly related to the changes of the electronic specific heat and a detailed comparison with specific-heat measurements is given. In Sec. IV we discuss the calculated local moments of the impurities, which are in good agreement with earlier estimates.[2,3] We stress the similarities and differences between the lo-

cal moments in Fe and Ni. The main results of the present paper, the magnetization distributions in the first five shells around the impurity, are given in Sec. V. In particular the change of the total magnetization per impurity atom is considered and a comparison with magnetization measurements is made. The general trend of these magnetization changes and the role of majority and minority bands in screening are quite different compared to the strong ferromagnets Ni and Co. In Sec. VI the main results are summarized.

II. THEORETICAL METHOD

In the calculations we employ density-functional theory in the local-density approximation. We use the local functional of von Barth and Hedin[13] but with the parameters as determined by Moruzzi *et al.*[14] (MJW). Only for *Fe*Mn are the results sensitive to the particular form of the exchange-correlation potential used (see discussion in Sec. IV).

Our calculations are based on multiple-scattering theory using the KKR Green's-function method, which we will outline shortly for paramagnetic systems; the generalization to magnetic systems is obvious. For more details we refer to Ref. 15. For lattice of muffin-tin potentials centered at positions $\mathbf{R}^n$ the Green's function can be expanded into eigensolutions of these spherically symmetric local potentials,

$$G(\mathbf{r}+\mathbf{R}^n,\mathbf{r}'+\mathbf{R}^{n'};E) = \sqrt{E}\,\delta_{nn'}\sum_L Y_L(\mathbf{r})H_L^n(r_>;E)R_l^n(r_<;E)Y_L(\mathbf{r}') + \sum_{L,L'} Y_L(\mathbf{r})R_l^n(r;E)G_{LL'}^{nn'}(E)R_{l'}^{n'}(r';E)Y_{L'}(\mathbf{r}') \; . \tag{1}$$

Here the vectors $\mathbf{r}$ and $\mathbf{r}'$ are restricted to the Wigner-Seitz cell and $r_>$ ($r_<$) denotes the larger (smaller) value of $r=|\mathbf{r}|$ and $r'=|\mathbf{r}'|$. The subscript $L=(l,m)$ collectively denotes the angular momentum quantum numbers l and m and $Y_L(r)$ are real spherical harmonics. The regular $[R_l^n(r;E)]$ and the irregular solutions $[H_l^n(r;E)]$ of the radial Schrödinger equation for the nth muffin-tin potential are defined by their asymptotic behavior outside the muffin-tin sphere of radius S,

$$\begin{aligned} R_l^n(r;E) &= j_l(\sqrt{E}r)+\sqrt{E}\,t_l^n(E)h_l(\sqrt{E}r) \; , \\ H_l^n(r;E) &= h_l(\sqrt{E}r), \quad \text{for } r\geq S \; , \end{aligned} \tag{2}$$

where j_l and h_l are the spherical Bessel and Hankel functions and $t_l^n(E)$ is the usual on-shell t matrix for the nth potential. Near the origin these functions behave as $R_l^n(r;E)\sim r^l$ and $H_l^n(r;E)\sim 1/r^{l+1}$.

All the information about the multiple scattering between the muffin tins is contained in the structural Green's-function matrix $G_{LL'}^{nn'}(E)$. It can be related to its counterpart $\mathring{G}_{LL'}^{nn'}(E)$ for the host crystal by an algebraic Dyson equation,

$$G_{LL'}^{nn'}(E)=\mathring{G}_{LL'}^{nn'}(E)+\sum_{n'',L''}\mathring{G}_{LL''}^{nn''}(E)\Delta t_{l''}^{n''}(E)G_{L''L'}^{n''n'}(E) \; . \tag{3}$$

The summation goes over all sites n'' and angular momenta L'' for which the perturbation $\Delta t_{l''}^{n''}(E)=t_{l''}^{n''}(E)-\mathring{t}_{l''}^{n''}(E)$ of the t matrices $\mathring{t}$ of the host is significant.

In the calculations we take s, p, d and f states (with angular momenta $l\leq 3$) into account. We allow the potentials of the first five shells around the impurity to be perturbed. In total these are 58 atoms surrounding the impurity. The potentials are assumed to be spherically symmetric inside the Wigner-Seitz sphere, i.e., we use volume-conserving, but slightly overlapping, atomic-sphere potentials. Using iteration techniques all potentials are calculated self-consistently. The Dyson equation (3), being in our case of rank 944×944, is solved using a group-theoretical decomposition into irreducible submatrices, the largest of rank 70×70. This reduces the computer time considerably.

The charge density is obtained from the Green's function by

$$n(\mathbf{r}) = -\frac{2}{\pi}\int^{E_F} dE\;\mathrm{Im}G(\mathbf{r},\mathbf{r};E) = -\frac{2}{\pi}\mathrm{Im}\int dz\;G(\mathbf{r},\mathbf{r};z) \; . \tag{4}$$

Since the Green's function is, as a function of the complex energy variable z, analytical on the whole physical sheet with the exception of the real axis, the energy integral can be transformed to a contour integral in the complex energy plane,[16,17] provided this contour ends at the Fermi energy E_F on the real axis. The contour integral can be very easily calculated with rather few energy points since for complex energies z the Green's function is rather structureless. In practice this also means a large saving of computer time.[15]

The changes of the integrated density of states $\Delta N(E)$ induced by the impurity can be calculated using a generalization of the Friedel sum rule to multiple-scattering problems given by Lloyd[18] and Lehmann,[19]

$$\Delta N(E)=\frac{1}{\pi}\sum_{n,L}[\delta_l^n(E)-\mathring{\delta}_l^n(E)] - \frac{1}{\pi}\mathrm{Im}\ln\det|\delta_{nn'}\delta_{LL'}-\mathring{G}_{LL'}^{nn'}(E)\Delta t_{l'}^{n'}(E)| \; , \tag{5}$$

where $\delta_l^n(E)$ are the scattering phase shifts. We use a generalization of this formula for complex energies.[20]

An important approximation in our calculations is that we neglect the lattice relaxations around the impurities, i.e., we fix the neighboring host atoms at the ideal lattice positions.

III. DENSITIES OF STATES AND SPECIFIC HEAT

Figure 1 shows the calculated local densities of states (DOS) in the impurity Wigner-Seitz sphere for the 3*d* impurities V, Cr, Mn, Co, and Ni together with the DOS of pure Fe, denoted by "Fe in Fe." In pure Fe the Fermi energy falls into a minimum of the minority-spin DOS. This minimum is typical for the DOS of bcc metals and separates the lower-lying bonding states from the higher antibonding ones. In the majority-spin band the Fermi

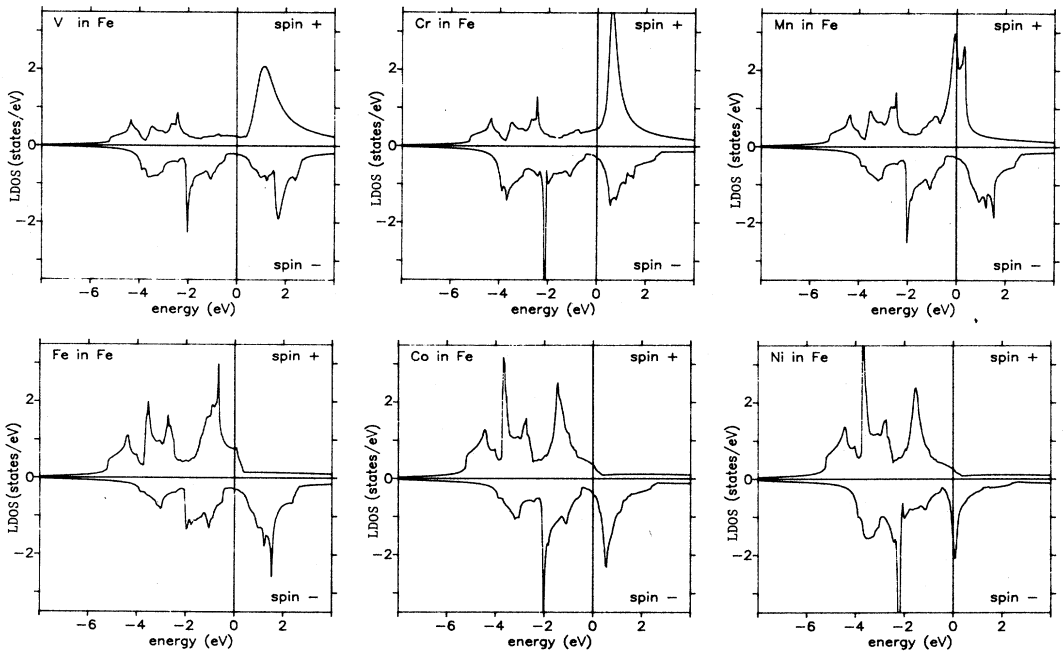

FIG. 1. Local densities of states of 3*d* impurities in Fe for both spin directions. The figure denoted "Fe in Fe" represents the density of states of pure Fe.

energy cuts off the upper shoulder from the *d* DOS so that about 0.2–0.3 *d* states are not occupied. This is the reason why the moment of pure Fe is only $2.15\mu_B$ and not $(2.5-2.7)\mu_B$ as one would expect for a "strong" ferromagnet with a filled majority-spin band. Therefore Fe is called a "weak" ferromagnet.

For Co and Ni impurities we observe the tendency that the local majority-spin DOS becomes more and more filled. In addition the minority states are also filled up to accommodate the additional charge. This leads to a large peak at the Fermi energy in the minority-spin DOS of the Ni impurity. In the case of Mn, Cr, and V impurities the population of the minority-spin DOS does not change very much. Here the major effect is the shift of the upper peak of the majority-spin DOS through the Fermi energy. This peak is just at E_F in the case of Mn and forms an empty virtual bound state above E_F for Cr and V. The local moments of the impurities, which can be directly calculated from the local DOS, are discussed in Sec. IV.

Unfortunately we are not aware of any photoemission experiments on these systems with which we could compare our results. The only information available about the density of states are specific-heat measurements.[21–23] As it is well known the electronic contribution to the specific heat is given by $c_e(T)=\gamma T$, where the coefficient γ is given by

$$\gamma=\frac{k_B^2\pi^2}{3}n(E_F)(1+\lambda)\ . \tag{6}$$

Here $n(E_F)$ is the DOS at the Fermi energy, k_B the Boltzmann constant, and λ is the mass enhancement which is normally due to electron-phonon interaction (see, e.g., Ref. 24). However, for ferromagnets electron-magnon interaction also seems to be very important. From the calculated DOS at E_F for pure Fe, $n(E_F)=1.04$ states/eV atom, and the measured value[21] of $\gamma=4.79$ (mJ/mol K^2) we estimate a mass enhancement of $\lambda_{\mathrm{Fe}}\cong 1.96$.

From Eq. (6) above we obtain for the relative changes of γ, $n(E_F)$, and λ in the alloy

$$\frac{\Delta\gamma}{\gamma}=\frac{\Delta n(E_F)}{n(E_F)}+\frac{\Delta\lambda}{1+\lambda}\ . \tag{7}$$

Since $\Delta\lambda$ is unknown, we compare in Figs. 2 and 3 the calculated relative changes $\Delta n(E_F)/n(E_F)$ directly with the values $\Delta\gamma/\gamma$ measured by several groups. All values refer to the changes arising from one impurity atom.

The changes $\Delta n(E_F)$ in Figs. 2 and 3 are calculated by summing up the changes of the impurity cell and of all Fe atoms in the first five shells around the impurity. Thus we have not summed up all changes up to infinite extent as would have been the case if Lloyd's formula for the integrated DOS were used and $\Delta n(E)$ were calculated by taking the derivative. Therefore the calculated changes might not be completely converged with respect to the number of shells included.

Nevertheless Fig. 2 clearly shows that our calculated local DOS resemble the qualitative trends found in the specific-heat experiments, i.e., the negative values for the early 3*d* impurities, the positive value for Mn followed by a negative one for Co and again a positive one for Ni. Unfortunately no measurements for Cu impurities exist. The dashed line in Fig. 2 shows the majority-spin band contribution $\Delta n^+(E_F)/n(E_F)$ compared to $\Delta n(E_F)$

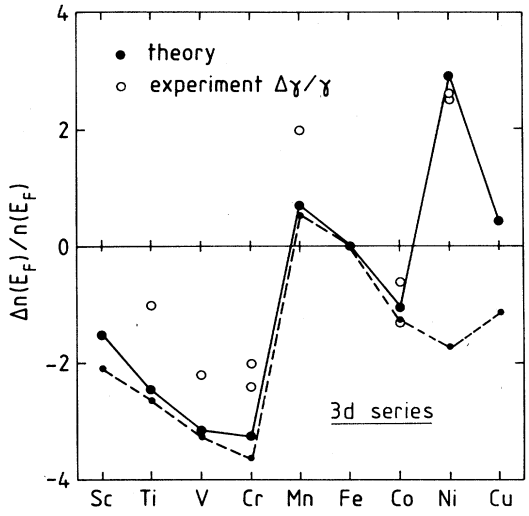

FIG. 2. Relative change $\Delta n(E_F)$ of the total density of states per $3d$ impurity atom compared to the density of states $n(E_F)$ per Fe atom in pure Fe [solid line, $\Delta n(E_F)/n(E_F)$]. The dashed curve shows the contribution $\Delta n^+(E_F)/n(E_F)$ from the majority-spin band. The circles give the relative change $\Delta\gamma/\gamma$ of the coefficients for the electronic specific heat as determined by experiment (Refs. 21–23).

$/n(E_F)$, where $\Delta n(E_F)=\Delta n^+(E_F)+\Delta n^-(E_F)$. One sees that except for Ni and Cu impurities all important contributions to $\Delta n(E_F)$ come from the majority-spin band. In these Fe alloys the DOS at E_F of the minority-spin band practically does not change with concentration, so that also for the more concentrated alloys the pronounced minimum of the minority-spin DOS at E_F is well preserved. This is fully in line with the arguments of Malozemoff *et al.*[25] that in ferromagnetic alloys, especially in Fe alloys, the Fermi energy is very likely fixed at a minimum of the DOS which then acts as a pseudogap. In Sec. V we will show that this behavior is of prime importance for the understanding of the magnetic properties of these alloys.

The qualitative trend shown in Fig. 2 can already be understood from the local DOS of the impurities as shown in Fig. 1. In the minority-spin band the minimum at E_F is for all impurities very much the same as for pure Fe. The only exception is Ni, where a sharp increase at E_F is observed due to the lowering of the upper peak. In the majority-spin band the situation is, however, very different. For V and Cr the upper edge of the host DOS is strongly reduced, for the impurities as well as for the the neighboring Fe atoms. This naturally arises from the hybridization of the host states with the upper virtual bound state of the impurities which pushes the Fe states to lower energies. For Mn the upper peak moves to the Fermi energy which explains the positive specific-heat values. On the other hand, for Co and Ni impurities the majority-spin band becomes more and more filled, so that $\Delta n^+(E_F)$ is negative. The large positive specific-heat value for Ni is totally due to the sharp peak at E_F in the minority-spin DOS.

In this context it is also noteworthy that Shinozaki and Arrot[21] find a nonlinear concentration dependence of γ in the case of dilute *Fe*Mn and *Fe*Ni alloys, whereas the alloys with Ti, V, Cr, and Co show a linear concentration dependence. This is in qualitative agreement with the local DOS in Fig. 1 since one expects the sharp Ni and Mn peaks at E_F to broaden rapidly with concentration.

IV. IMPURITY MOMENTS

The calculated local moments of the $3d$ and $4d$ impurities in Fe are shown in Figs. 4 and 5, together with the

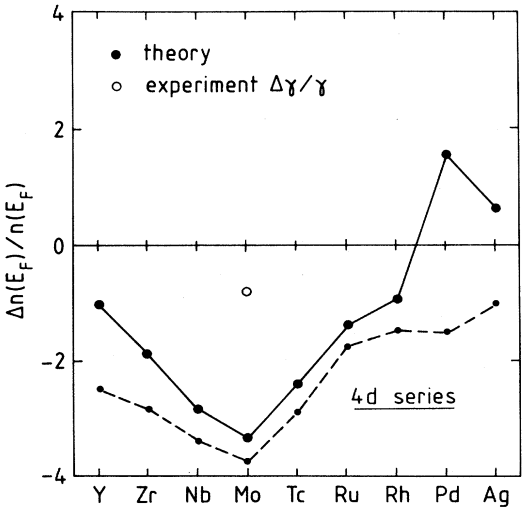

FIG. 3. Relative change $\Delta n(E_F)/n(E_F)$ for $4d$ impurities [experiment, Mo (Ref. 21)] (same nomenclature as in Fig. 2).

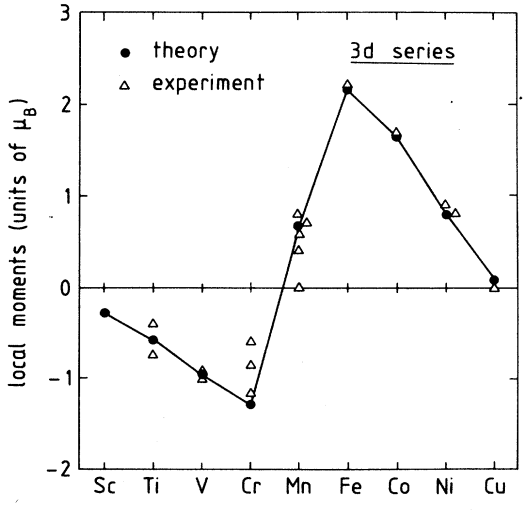

FIG. 4. Local moments in the impurity Wigner-Seitz sphere for $3d$ impurities in Fe. The triangles are experimental values from neutron scattering [Ti (Refs. 27 and 29), V (Refs. 21 and 33), Cr (Refs. 29, 31, and 32), Mn (Refs. 27–30), Co (Ref. 26), Ni (Refs. 27 and 29), Cu (Ref. 34)].

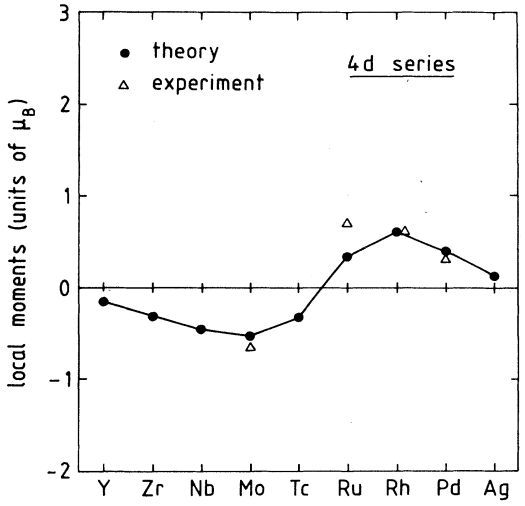

FIG. 5. Local moments in the impurity Wigner-Seitz sphere for 4*d* impurities in Fe. The triangles are experimental values from neutron scattering (Refs. 29 and 53).

experimental data obtained by neutron scattering.[26–34] In general the agreement with the experimental data is very good. The early 3*d* impurities couple antiferromagnetically to the host atoms whereas the late ones, Mn, Co, and Ni, couple ferromagnetically. This behavior is very similar to the one found in Ni (Refs. 35 and 36) and is well understood from the work of Friedel,[37] Kanamori,[38] and Campbell and Gomes.[39] The moments found for the 4*d* impurities are in general much smaller than the ones in the 3*d* series. The same trends are also found in Ni. However, there are some subtle differences between 3*d* impurities in Ni and Fe which we will discuss below.

Compared with the calculations of Akai *et al.*,[2] which are based on a single-site approximation for the perturbed potentials, the present results for the antiferromagnetic impurities Ti, V, and Cr, are in much better agreement with the experimental data. Here the inclusion of the perturbed neighboring potentials is essential as has been found already in a previous publication.[3]

The local moment of the Mn impurity turns out to be sensitive to the special form of the exchange-correlation potential used in the calculation. While the MJW local functional[14] and the one of Vosko, Wilk and Nusair (VWN) (Ref. 40) yield similar values of $0.69\mu_B$ and $0.64\mu_B$, respectively, the one of von Barth and Hedin[13] (vBH) gives rise to a considerably smaller value ($0.34\mu_B$). The VWN potential is generally believed to be somewhat more accurate, since it is based on exact results for the homogeneous electron gas. From Fig. 1 it is seen that the values calculated either with the MJW or VWN local functional are in good agreement with the experimental data. In this context it should be noted that the negative values reported for the Mn moment by Kajzar and Parette[41] are unreliable. These results show an unreasonably large concentration dependence and are in disagreement with other experimental findings.[27–30] The same authors also obtained unreasonably large negative values for the moments of Cr, V, and Ti (Refs. 41 and 42) which are not included in Fig. 4.

For 3*d* impurities in Ni, Zeller[35] found in calculations for noninteger nuclear charges Z that there exists a rather broad region of Z values, $24 \leq Z \leq 26$, where the ferromagnetic and antiferromagnetic solution are stable or metastable, respectively. Contrary for Fe, Akai *et al.*[2] found no such transition region and a negative moment of $-1.7\mu_B$ for Mn, whereas Anisimov *et al.*[5] report a positive ($1.6\mu_B$) and a negative moment ($-2.3\mu_B$) for Mn, both corresponding to stable solutions. Our calculations indicate that Mn in Fe is a very critical case. It is not only sensitive to the exchange-correlation potential used but also to other approximations made in the calculation, especially the angular momentum cutoff. In an $l \leq 2$ calculation we find for the MJW potential a sharp and discontinuous (first order) transition at $Z = 25.04$ from the ferromagnetic to the antiferromagnetic solution, in agreement with Akai *et al.*[2] Both for the vBH and VWN potentials the same transition occurs in an $l \leq 2$ calculation for nuclear charges Z slightly smaller than 25, the transition itself is however smoother and continuous (second order). In a more accurate $l \leq 3$ calculation these transitions are shifted to smaller Z values and a positive moment is obtained for all three exchange-correlation potentials.

The major difference between the behavior of 3*d* impurities in Ni and Fe is therefore the existence of a relatively large two-state region in Ni, which is absent in Fe. We will now give a plausibility argument that this is a direct consequence of the much larger host moment of Fe. In nonmagnetic hosts, e.g., in Cu, 3*d* impurities such as Cr, Mn, or Fe have a stable magnetic moment M_0. As a function of the nuclear charge Z, this moment M_0 varies as shown in Fig. 6(a), with the maximum occurring at Mn. With respect to an arbitrary quantization axis, also the state with moment $-M_0$ exists and is degenerate with $+M_0$. In a plot of the total energy $E(M)$ as a function of the hypothetically varying moment M we expect a symmetrical curve with two well-defined minima at $\pm M_0$ [Fig. 6(b)]. The maximum at $M = 0$ corresponds to the paramagnetic state [dashed line in Fig. 6(a)]. If we now consider a ferromagnetic host with a rather small host moment, such as Ni, we expect that for Mn the two minima still exist, but that the degeneracy is broken and one minimum is slightly lower than the other one [Fig. 6(d)]. This is plausible since the impurity moment is much larger than the host moment. By varying the nuclear charge and considering M_0 as a function of Z, we obtain a curve as shown in Fig. 6(c). For the late 3*d* impurities only the ferromagnetic state survives, for the early ones only the antiferromagnetic one, whereas in the middle of the series two states exist. This just corresponds to the results for Ni found by Zeller.[35] The dashed line in Fig. 6(c) is the solution corresponding to the maximum. If we then consider a host with a larger moment, we obtain a case where even in the middle of the series the second minimum disappears [Fig. 6(f)]. In this case the $M_0(Z)$ curves suddenly, but continuously drops in the middle of the series from positive to negative values [Fig. 6(e)]. This is just the situation which we and Akai *et al.*[2] found

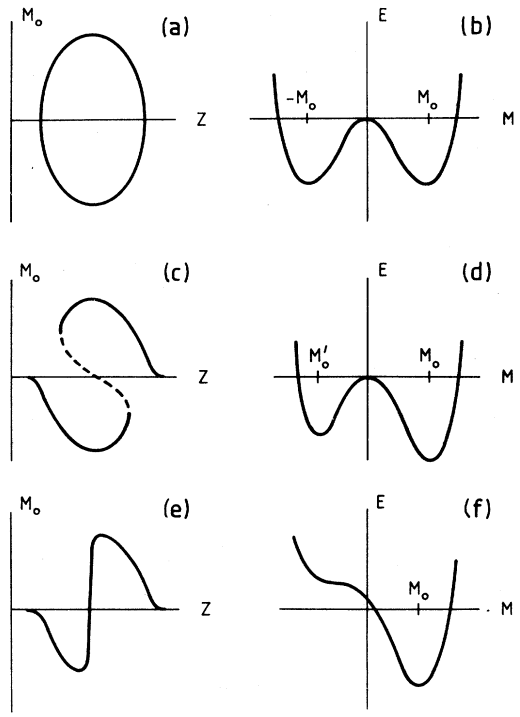

FIG. 6. Schematic behavior for the total energy E as a function of the variable impurity moment M and for the real impurity moment M_0 as a function of the atomic number Z. (a) and (b) refer to 3d impurities in a paramagnetic host like, e.g., Cu, (c) and (d) refer to a ferromagnet with a small host moment like Ni, and (e) and (f) refer to a ferromagnet with a larger moment like Fe.

to occur close to Mn in Fe. This sharp transition explains why Mn in Fe is such a difficult case. Contrary to 3d impurities, 4d impurities are not magnetic. Consequently we expect, in a ferromagnetic host, that the $E(M)$ function has only one minimum. The $M_0(Z)$ curve should then be rather flat and S shaped, which is what we have found in Fig. 4 for the local moments. It is then more appropriate to speak of an induced moment, i.e., one which is induced on the impurity site by the host polarization.

V. MAGNETIZATION OSCILLATIONS

The calculated magnetization changes ΔM_n ($n=1,2,\ldots,5$) for Fe atoms in the first five shells around the impurities are listed in Table I for the 3d series and in Table II for the 4d series. Given are also the changes $\Delta M_{\rm cl}$ of the total magnetization obtained by summing up the local changes of the impurity cell and of the Fe atoms in the first five shells. Alternatively the changes of the total magnetization can be calculated using Lloyd's formula, thereby including also longer-ranged contributions. This leads to the values denoted by ΔM. The difference between $\Delta M_{\rm cl}$ and ΔM gives an indication whether the considered cluster of perturbed potentials is sufficiently large to include all magnetization perturbations.

Figures 7 and 8 show the total change ΔM of the magnetization per impurity for the 3d and 4d series, together with experimental data.[43–56] ΔM is also often referred to as the concentration derivative of the magnetization in the dilute limit, i.e., $\Delta M = dM/dc|_{c=0}$, where c is the atomic concentration. The general trend found experimentally, i.e., the increase of the magnetization for Co, Ni, and Rh,Pd as well as the strong negative decrease of the magnetization towards the beginning of the series are well reproduced by the calculations. A closer look at the figure reveals that the calculated data are on the average somewhat below the experimental points. While in some cases like Ru, Rh, and Pd this is not significant due to the large uncertainties of the experiments, the data for Ti, V, and Cr as well as Mo seem to be sufficiently reliable and indicate that there might be a problem with the calculations. For these impurities Table I shows a relatively large difference between the change $\Delta M_{\rm cl}$ of the moment in the cluster and the value ΔM calculated by Lloyd's formula. This points to positive contributions to ΔM from shells further away. Though by using Lloyd's formula, Eq. (5), these contributions are formally included in ΔM, they are not entering the self-consistency cycle and are therefore presumably underestimated. The relatively good agreement between ΔM and $\Delta M_{\rm cl}$ for the late transition-metal impurities shows that these uncertainties due to the restricted number of perturbed atoms only occur for the early d impurities.

Let us now discuss the shell dependence of the changes

TABLE I. Local moments M_0 of 3d impurities in Fe. The values ΔM_n are the changes of the local moment of an Fe atom in the nth shell around the impurity. $\Delta M_{\rm cl}$ is the change of the total moment summed over the impurity and five shells of Fe atoms; ΔM is essentially the same quantity, but calculated by Lloyd's formula. The results have been obtained using the MJW exchange-correlation potential.

	M_0/μ_B	$\Delta M_1/\mu_B$	$\Delta M_2/\mu_B$	$\Delta M_3/\mu_B$	$\Delta M_4/\mu_B$	$\Delta M_5/\mu_B$	$\Delta M_{\rm cl}/\mu_B$	$\Delta M/\mu_B$
Sc	−0.29	−0.204	−0.069	−0.011	−0.005	+0.036	−4.46	−4.19
Ti	−0.58	−0.173	−0.040	−0.002	−0.006	+0.046	−4.15	−3.86
V	−0.96	−0.118	−0.019	+0.013	−0.003	+0.050	−3.69	−3.37
Cr	−1.29	−0.067	−0.012	+0.028	+0.002	+0.049	−3.29	−2.93
Mn	+0.69	−0.057	−0.033	+0.018	+0.004	+0.027	−1.78	−1.51
Fe	+2.16	0	0	0	0	0	0	0
Co	+1.65	+0.098	+0.025	+0.007	+0.009	+0.009	+0.79	+0.72
Ni	+0.79	+0.114	+0.025	+0.013	+0.014	+0.011	+0.28	+0.22
Cu	+0.08	+0.019	−0.013	−0.005	+0.009	−0.003	−1.86	−1.92

TABLE II. Local moments M_0 of 4*d* impurities in Fe and changes ΔM_n of the Fe moments in the *n*th shell around the impurity. The same nomenclature as in Table I is used.

	M_0/μ_B	$\Delta M_1/\mu_B$	$\Delta M_2/\mu_B$	$\Delta M_3/\mu_B$	$\Delta M_4/\mu_B$	$\Delta M_5/\mu_B$	$\Delta M_{cl}/\mu_B$	$\Delta M/\mu_B$
Y	−0.16	−0.213	−0.046	+0.026	+0.012	+0.047	−3.36	−3.02
Zr	−0.31	−0.225	−0.053	+0.022	+0.004	+0.054	−3.81	−3.42
Nb	−0.46	−0.210	−0.040	+0.029	+0.002	+0.059	−3.68	−3.26
Mo	−0.52	−0.180	−0.033	+0.041	+0.001	+0.059	−3.31	−2.86
Tc	−0.32	−0.121	−0.040	+0.050	+0.002	+0.050	−2.65	−2.21
Ru	+0.34	−0.016	−0.033	+0.045	+0.007	+0.030	−1.20	−0.93
Rh	+0.60	+0.073	+0.006	+0.040	+0.015	+0.011	−0.01	+0.06
Pd	+0.40	+0.109	+0.021	+0.034	+0.021	+0.011	+0.25	+0.20
Ag	+0.06	−0.002	−0.018	+0.012	+0.016	+0.001	−1.70	−1.75

ΔM_n of the local moments (see Tables I and II). Figures 9 and 10 show the total change ΔM (solid line), the contribution to ΔM from the impurity cell (dashed line), and the sum of the contributions from the impurity and the first shell atoms (dotted line). From these curves and from Tables I and II one finds that the magnetization changes ΔM_n show a rather complicated behavior. For Co and Ni the local impurity moments decrease compared to Fe, but the moments of all Fe atoms in the five shells around the impurity increase. Thus we have an extended positive polarization cloud around the impurity and the decrease of the local moment is more than compensated by the increase of the surrounding host moment. These alloys show a tendency towards strong ferromagnetism with a partial filling up of the majority-spin band (see below and Sec. II). A similar behavior is also found for the isoelectronic 4*d* impurities Rh and Pd. While the local impurity moments are much smaller, the positive polarization clouds are equally extended and carry even larger moments.

The early transition-metal impurities show a more complicated behavior. In the sequence $_{24}$Cr to $_{21}$Sc and $_{42}$Mo to $_{39}$Y the local moments of these impurities decrease more or less linearly, which is similar to the behavior found in Ni. On the other hand, the total change ΔM increases almost linearly, which is in strong contrast to the behavior found[57] in Ni, where ΔM decreases in this sequence according to $\Delta M \cong -10-\Delta Z$. Thus the global

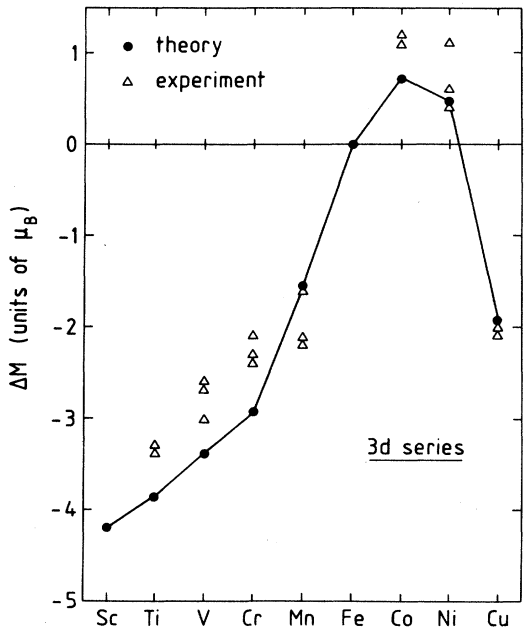

FIG. 7. Total change ΔM of the magnetization per impurity atom as calculated for 3*d* impurities in Fe. The triangles are the results of magnetization measurements [Ti (Refs. 43 and 44), V (Refs. 33, 45, and 46), Cr (Refs. 44, 46, and 47), Mn (Refs. 28, 30, 44, and 48), Co (Refs. 44 and 49), Ni (Refs. 44, 50, and 51), Cu (Refs. 35 and 52)].

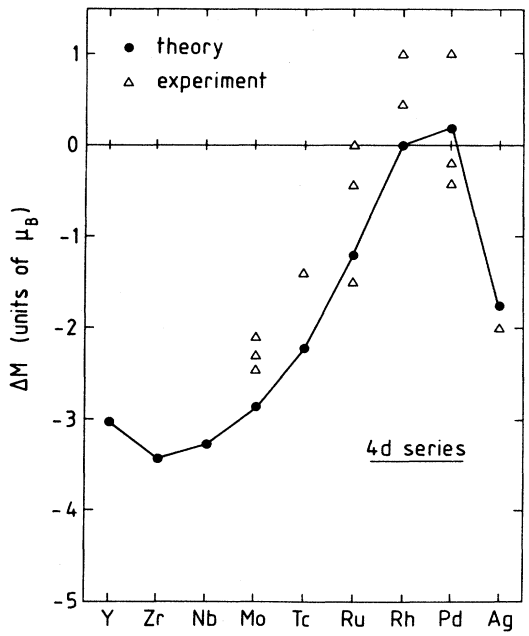

FIG. 8. Total change ΔM of the magnetization for 4*d* impurities [△, experiments; Mo (Refs. 48, 52, and 53), Tc (Ref. 52), Ru (Refs. 44, 53, and 54), Rh (Refs. 44 and 54), Pd (Refs. 44, 54, and 55), Ag (Ref. 56)].

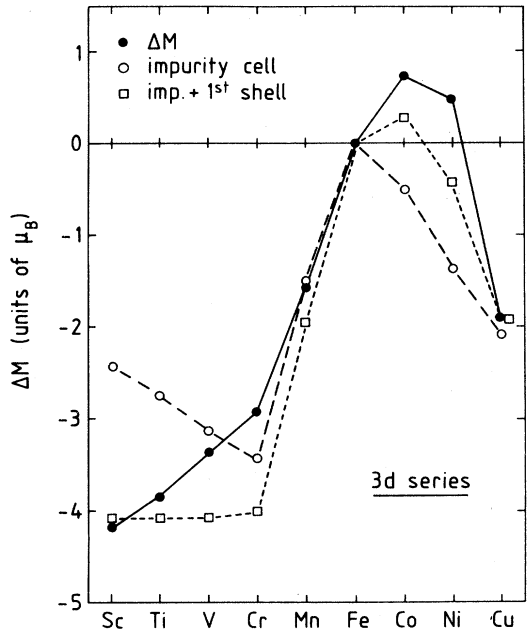

FIG. 9. Contributions to the total change ΔM of the magnetization (●) due to 3*d* impurities (○, contribution from the impurity cell; □, sum of the contributions from the impurity cell and first-shell atoms).

behavior of the magnetization in Fe is quite different from the local impurity behavior, both for the early as well as late transition-metal impurities. Moreover the polarization clouds of the early 3*d* impurities show a lot of structure. While the contributions from the first two shells are strongly negative, the ones from the third, fourth, and fifth shells are positive, with the fourth one giving only a minor contribution. Presumably some more positive contributions come from atoms further away which are not explicitly included in the self-consistency.

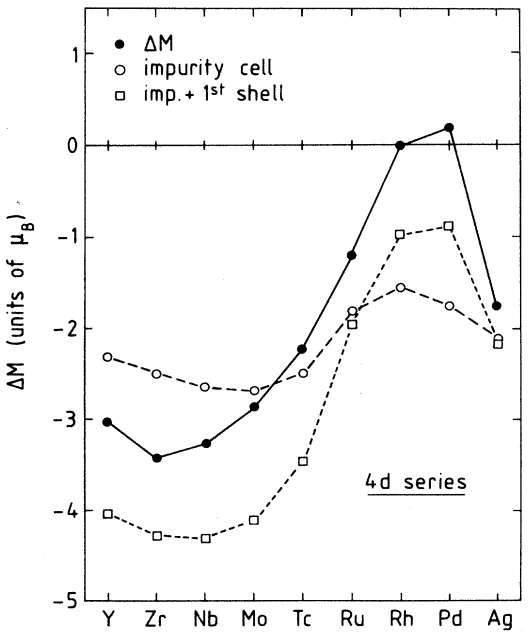

FIG. 10. Contributions to the total change ΔM of the magnetization due to 4*d* impurities (same nomenclature as in Fig. 9).

The only direct information about the magnetization disturbances around the impurities can be obtained by magnetic neutron scattering. Campbell[53] has analyzed the earlier experiments of Collins and Low[29] in detail. Within the experimental uncertainty it is not possible to distinguish between the moments of the first and second neighbors as well as between the moments of the third, fourth, and fifth neighbors. For the average moments of the first and second neighbors he obtains positive moments for Co and Ni as well as for Rh and Pd and negative values for the early 3*d* impurities as well as for Mo and Ru. Within the relatively large experimental uncertainties, these values agree with our calculated data. The average moments for the third-, fourth-, and fifth-shell atoms are always positive. Both the signs and magnitudes of these data agree with our results. This is also true for the results obtained by Child and Cable[27] for *Fe*Mn and by Aldred *et al.*[31] for *Fe*Cr. However, our results strongly disagree with the experiments of Kajzar and Parette[41,42] for *Fe*Mn, *Fe*Cr, *Fe*V, and *Fe*Ti. These authors obtain relatively large positive changes for the first neighbors which are incompatible with our calculations as well as with the above experimental results. A much more meaningful comparison with the neutron-scattering results would require to calculate the cross sections for magnetic scattering directly. This is, however, beyond the scope of the present paper.

The total change ΔM of the magnetization can be expressed by the global changes $\Delta N^{\pm}(E_F)$ of the populations of the majority-spin (+) and minority-spin bands (−) which are calculated by Lloyd's formula. $\Delta M = \Delta N^{-}(E_F) - \Delta N^{-}(E_F)$ is the difference of these population changes whereas the sum $\Delta N^{+}(E_F) + \Delta N^{-}(E_F) = \Delta Z$, the change of the impurity nuclear charge, if the Friedel sum rule is satisfied exactly. As has been emphasized recently by Williams *et al.*[12,25] these populations $\Delta N^{\pm}(E_F)$ show a very simple behavior if the alloys are strong ferromagnets. Then the majority-spin band remains filled, i.e., $\Delta N^{+}(E_F) = 0$ and the magnetization changes opposite to the valence: $\Delta M = -\Delta Z$. In Ni these relations are very well satisfied for Co, Fe, and Mn impurities as well as for the early 4*sp* impurities (Cu, Zn, Ga).[57] Contrary for the early 3*d* impurities in Ni a *d* virtual bound state moves above the Fermi energy in the majority-spin band, so that $\Delta N^{+}(E_F) = -5$ and $\Delta M = -10 - \Delta Z$. Our calculations[57] have shown that these relations are well satisfied in Ni.

Contrary to Ni, in Fe, where the majority-spin band is nearly filled (about 0.2–0.3 electron are missing), the situation is very different, as shown in Figs. 11 and 12. Instead, here the minority-spin band population is more or less constant, while the majority-spin band population changes about linearly with ΔZ. This is also in agreement with the results for the change $\Delta n(E_F)$ of the total DOS as discussed in Sec. III. Figure 2 clearly shows that, with the exception of Ni, all the action is in the

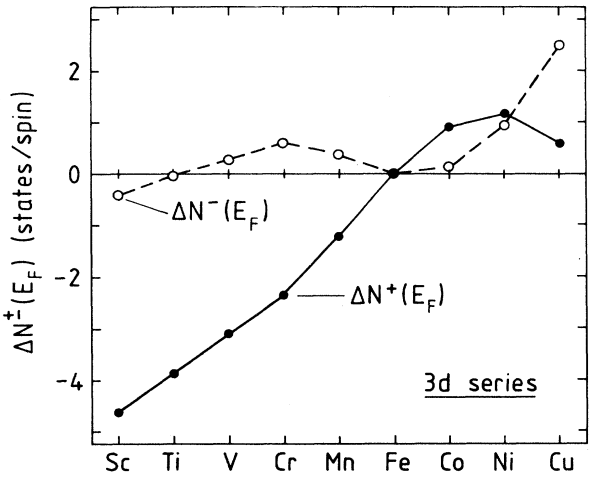

FIG. 11. Change of the integrated densities of states $\Delta N^{\pm}(E_F)$ for both spin directions in the case of $3d$ impurities. $\Delta N^{+}(E_F)$ gives the change of the majority-spin band population, and $\Delta M^{-}(E_F)$ that of the minority-spin band. Note that $\Delta Z = \Delta N^{+}(E_F) + \Delta N^{-}(E_F)$ if the Friedel sum rule were exactly satisfied (see Table II).

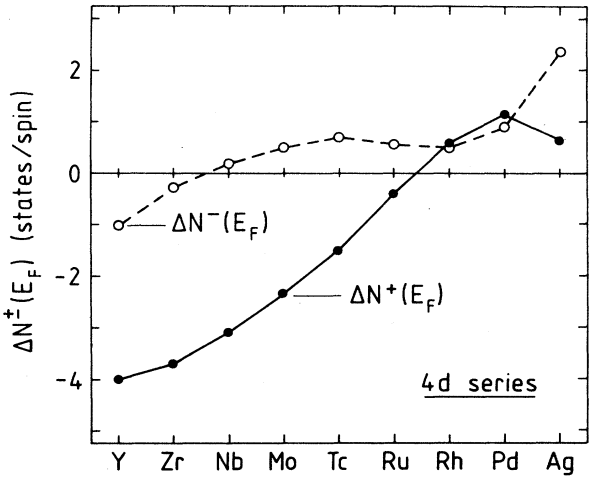

FIG. 12. Change $\Delta N^{\pm}(E_F)$ for the case of $4d$ impurities in Fe (same nomenclature as in Fig. 11).

majority-spin band. Thus in Fe the role of both subbands is exchanged compared to Ni and Co. Such a behavior has been discussed by Malozemoff *et al.*[25] in their "gap theory" for ferromagnetic alloys. The main argument is that if the paramagnetic Fermi energy lies close to a minimum of the density of states then the Fermi energy of the ferromagnetic alloy is very likely to be pinned in this minimum. Indeed we have seen in Sec. III that also in the dilute alloys the minimum in the minority DOS at E_F is well preserved and no new states appear in the "gap" region of the DOS. Only at the end of the $3d$ series (Ni) do the edges of the antibonding peak move to the Fermi energy. This naturally explains why in Fe the majority-spin band contributes most of the screening. Nevertheless the variation of the minority-spin population, though smaller than the majority-spin one, cannot be completely neglected. Otherwise ΔM would vary as $\Delta M = -\Delta Z$ which is clearly not the case (see Fig. 7). This is a direct consequence of the fact that the Fermi energy lies merely in a minimum of the DOS, but not in a true gap.

VI. SUMMARY

In our *ab initio* calculations we calculate both the local properties of the $3d$ and $4d$ impurities in Fe as well as the changes of the global properties arising from the induced host perturbations. We employ the local-density approximation together with the KKR Green's function method. The impurity potential and the perturbed potentials for five shells of Fe atoms are determined self-consistently.

The calculated impurity moments are in very good agreement with data from neutron scattering. Contrary to previous results, but in agreement with the experiments, we obtain for Mn a positive moment. We show that Mn in Fe is a difficult case, since the moment of Mn in Fe is close to the transition from a ferromagnetic to an antiferromagnetic coupling with the host moments.

The calculated changes of the total density of states at the Fermi energy agree well with specific-heat measurements. Except for Ni in Fe all trends are determined by the variation of the DOS of the majority-spin band, showing that the minimum of the DOS in the minority-spin band is well preserved in these alloys.

For Co and Ni as well as for Rh and Pd impurities we obtain a long-ranging enhancement of the neighboring Fe moments, indicating a tendency towards strong ferromagnetism in these alloys. For the early transition-metal impurities a more complicated oscillatory behavior of the neighboring Fe moments is found. Strong negative contributions from the atoms in the first two shells exist together with positive contributions from the atoms further away. These results are in qualitative agreement with the limited information from neutron scattering.

The calculated changes of the total moment are compared with magnetization measurements. In general the agreement is good, but there are some systematic deviations for the early d impurities which presumably arise from the neglect of a self-consistent treatment of the atoms beyond the fifth shell. The analysis of the majority- and minority-spin band populations shows that the changes in the majority-spin band are much larger than in the minority-spin band. Thus contrary to the strong ferromagnetic Co and Ni alloys the majority-spin band contributes most of the screening in these Fe alloys. The physical reason for this fact is that the Fermi energy lies in the minimum of the minority-spin DOS of Fe. Since this minimum is well preserved in the dilute alloys

it acts as a pseudogap[25] and tends to keep the number of occupied states in the minority-spin band approximately constant. This is the reason for the rather complicated magnetic behavior of the Fe–transition-metal alloys.

ACKNOWLEDGMENTS

It is a pleasure to thank H. Akai and M. Weinert for many discussions and for their help in performing the calculations.

---

*Present address: Division of Solid State Physics, Physics Department, University of Athens, Athens, Greece.

†Present address: The Institute of Solid State Physics, University of Tokyo, 3-2-1 Midori-cho, Tanashi, Tokyo 188, Japan.

[1]M. Akai, H. Akai, and J. Kanamori, J. Phys. Soc. Jpn. **54**, 4242 (1985); **56**, 1064 (1987).

[2]H. Akai, M. Akai, and J. Kanamori, J. Phys. Soc. Jpn. **54**, 4257 (1985).

[3]H. Akai, M. Akai, S. Blügel, R. Zeller, and P. H. Dederichs, J. Magn. Magn. Mater. **45**, 291 (1984).

[4]P. Leonard and N. Stefanou, J. Phys. (Paris) **43**, 1497 (1982); Philos. Mag. **51**, 151 (1985).

[5]V. Anisimov, V. Antropov, A. Liechtenstein, V. Gubanov, and A. Postnikov, Phys. Rev. B **37**, 5598 (1988).

[6]H. Hasegawa and J. Kanamori, J. Phys. Soc. Jpn. **31**, 382 (1971); **33**, 1599 (1972); **33**, 1606 (1972).

[7]D. D. Johnson, F. J. Pinsky, and G. M. Stocks, J. Appl. Phys. **57**, 3018 (1985).

[8]H. Akai, J. Phys. Condens. Matter (to be published).

[9]D. D. Johnson, F. J. Pinsky, and J. B. Staunton, J. Appl. Phys. **61**, 3715 (1987).

[10]H. Akai, P. H. Dederichs, and J. Kanamori, J. Phys. (Paris) Colloq. **49**, C8-23 (1988).

[11]S. Chikazumi, *Physics of Magnetism* (Wiley, New York, 1964), p. 74.

[12]A. R. Williams, V. L. Moruzzi, A. P. Malozemoff, and K. Terakura, IEEE Trans. Magn. **MAG-19**, 1983 (1983); A. P. Malozemoff, A. R. Williams, K. Terakura, V. L. Moruzzi, and K. Fukamichi, J. Magn. Magn. Mater. **35**, 192 (1983).

[13]U. von Barth and L. Hedin, J. Phys. C **5**, 1629 (1972).

[14]V. L. Moruzzi, J. F. Janak, and A. R. Williams, *Calculated Electronic Properties of Metals* (Pergamon, New York, 1978).

[15]P. J. Braspenning, R. Zeller, A. Lodder, and P. H. Dederichs, Phys. Rev. B **29**, 703 (1984).

[16]R. Zeller, J. Deutz, and P. H. Dederichs, Solid State Commun. **44**, 993 (1982).

[17]A. R. Williams, P. J. Feibelman, and N. D. Lang, Phys. Rev. B **26**, 5433 (1982).

[18]P. Lloyd, Proc. Phys. Soc. London **90**, 207 (1967); **90**, 217 (1967).

[19]G. Lehmann, Phys. Status Solidi B **70**, 737 (1975).

[20]B. Drittler, M. Weinert, R. Zeller, and P. H. Dederichs, Phys. Rev. B **39**, 930 (1989).

[21]S. S. Shinozaki and A. Arrot, Phys. Rev. **152**, 611 (1966).

[22]C. H. Chen, C. T. Wei, and P. A. Beck, Phys. Rev. **120**, 426 (1960).

[23]J. H. M. Stoelinga, G. de Vries, and F. J. Du Chatenier, Phys. Lett. **14**, 6 (1965).

[24]G. Grimvall, Phys. Scr. **14**, 63 (1976).

[25]A. P. Malozemoff, A. R. Williams, and V. L. Moruzzi, Phys. Rev. B **29**, 1620 (1984).

[26]M. F. Collins and J. B. Forsyth, Philos. Mag. **8**, 401 (1963).

[27]H. R. Child and J. W. Cable, Phys. Rev. B **13**, 227 (1976).

[28]Y. Nakai and N. Kunitorni, J. Phys. Soc. Jpn. **39**, 1257 (1975).

[29]M. F. Collins and G. G. Low, Proc. Phys. Soc. London **86**, 535 (1965).

[30]P. Radhakrishna and F. Livet, Solid State Commun. **25**, 597 (1978).

[31]A. T. Aldred, B. D. Rainford, J. S. Kouvel, and T. J. Hicks, Phys. Rev. B **14**, 228 (1976).

[32]C. G. Shull and M. K. Wilkinson, Phys. Rev. **97**, 304 (1955).

[33]I. Mirebeau, G. Parette and J. W. Cable, J. Phys. F **17**, 191 (1987).

[34]F. Kajzar and G. Parette, J. Appl. Phys. **50**, 1966 (1979).

[35]R. Zeller, J. Phys. F **17**, 2123 (1987).

[36]S. Blügel, H. Akai, R. Zeller, and P. H. Dederichs, Phys. Rev. B **35**, 3271 (1987).

[37]J. Friedel, Nuovo Cimento **10**, 287 (1958).

[38]J. Kanamori, J. Appl. Phys. **16**, 929 (1965).

[39]I. A. Campbell and A. A. Gomes, Proc. Phys. Soc. London **91**, 319 (1967).

[40]S. H. Vosko, L. Wilk, and M. Nusair, J. Can. Phys. **58**, 1200 (1980).

[41]F. Kajzar and G. Parette, Phys. Rev. B **22**, 5471 (1980).

[42]F. Kajzar and G. Parette, Solid State Commun. **29**, 323 (1979).

[43]A. T. Aldred, J. Phys. C **1**, 244 (1968).

[44]A. Arrott and J. E. Noakes, *Iron and its Dilute Alloys,* edited by P. A. Beck (Interscience, New York, 1963), p. 81.

[45]A. T. Aldred, Int. J. Magn. **2**, 223 (1972).

[46]M. C. Cadeville (private communication).

[47]A. T. Aldred, Phys. Rev. B **14**, 219 (1976).

[48]S. Arajs, Phys. Status Solidi **31**, 217 (1969).

[49]B. I. Bardos, J. Appl. Phys. **40**, 1371 (1969).

[50]J. Crangle and G. C. Hallam, Proc. R. Soc. London, Ser. A **272**, 119 (1963).

[51]M. Peschard, Rev. Metall. **22**, 581 (1925).

[52]A. T. Aldred, J. Phys. C **1**, 1103 (1968).

[53]I. A. Campbell, Proc. Phys. Soc. London **89**, 71 (1966).

[54]M. Fallot, Ann. Phys. (Paris) **10**, 291 (1938).

[55]M. B. Stearns, Phys. Rev. B **13**, 1183 (1976).

[56]K. Sumiyama and Y. Nakamura, Phys. Status Solidi A **81**, K109 (1984).

[57]N. Stefanou, A. Oswald, R. Zeller, and P. H. Dederichs, Phys. Rev. B **35**, 6911 (1987).